A Fourier Analysis Dynamic Birefringence Apparatus

SATISH KUMAR* and R. S. STEIN, *Polymer Research Institute and Materials Research Laboratory, University of Massachusetts, Amherst, Massachusetts 01003*

Synopsis

Molecular motion in a polymeric system can be studied using dynamic birefringence. Computer interfacing of the dynamic birefringence apparatus and the data treatment using Fourier analysis are reported in this paper. Experiments are done under sinusoidal strain; stress, strain and birefringence signals are monitored. Birefringence is measured using the optical transmission technique. An AIM-65 microcomputer was interfaced with this apparatus for the purposes of data acquisition and data analysis. First-order Fourier coefficients are used to determine the real and imaginary components of the modulus, the strain optical coefficient, and the stress optical coefficient. Higher order Fourier coefficients can be used to study the nonlinear viscoelastic behavior in the polymer.

INTRODUCTION

Several methods are used to understand the mechanism of molecular motion in polymers. Some of the prominent techniques are dynamic mechanical tests, dielectric studies, NMR, dynamic light and X-ray scattering, dynamic infrared spectroscopy, and dynamic birefringence. Dynamic mechanical and dielectric tests are the most extensively used techniques for the study of molecular dynamics. Developments in the field of dynamic light[1-3] and X-ray scattering,[4-6] dynamic infrared spectroscopy,[7,8] and dynamic birefringence[9-22] are relatively limited. It is highly unlikely that in any polymer information revealed by all these techniques will be the same. Certain mechanisms of molecular motion may be revealed by a number of techniques, while others may be more sensitive to one test and comparatively less or not at all sensitive to others. Read[17] has shown for poly(methyl methacrylate) that dynamic mechanical tests would only show a single relaxation process in the β region, but a dynamic mechanical test complemented by a dynamic birefringence test reveals that there are two relaxation processes (in the β region of PMMA) rather than one (Fig. 1 of reference 17). In a study on polyacrylonitrile, it was found that NMR is sensitive only to the lower of the two principal mechanical transitions.[23] These examples help to illustrate the fact that in order to understand the mechanism of molecular motion well enough, one must perform the tests using more than one technique.

The previous methods for measuring dynamic birefringence are (i) stroboscopic technique,[14] (ii) Lissajou figure technique,[9,10] and (iii) π-sector technique.[24]

*Present address: University of Dayton Research Institute, Dayton, OH 45469.

Journal of Applied Polymer Science, Vol. 34, 1693–1701 (1987)
 CCC 0021-8995/87/041693-09$04.00

Recently we have interfaced a microcomputer (AIM-65) to our dynamic birefringence apparatus for the purposes of data acquisition and data analysis. The data analysis is done using Fourier analysis. The instrumental development is reported in this paper. This apparatus has been used to study the dynamic birefringence behavior of acrylonitrile copolymers, findings of which are reported in the following publication.[25]

THEORY

Fourier Analysis

A periodic function can be expressed in terms of a Fourier series, as

$$Y(t) = Y^0 + \sum_{k=1}^{m} \Delta Y_k^*(i\omega)e^{i\omega kt} \tag{1}$$

where ΔY_k^* are Fourier coefficients, given by

$$\Delta Y_k^*(i\omega) = \frac{2}{m} \sum_{k=1}^{m} Ye^{2\pi ik(l-1)/m} \tag{2}$$

The first-order Fourier coefficient is given by

$$Y_1^* = Y^0 + Y_1'\sin\omega t + iY_1''\cos\omega t \tag{3}$$

For more than one signal, eq. (3) can be generalized as

$$Y_1^{j*} = Y^0 + Y_1^{j'}\sin\omega t + iY_1^{j''}\cos\omega t \tag{4}$$

where $j = 1$, 2, or 3 for strain, stress, and birefringence in the present case. If the strain signal is given by

$$\epsilon = \epsilon_0\sin(\omega t + \theta)$$

$$= \epsilon'\sin\omega t + \epsilon''\cos\omega t \tag{5}$$

where

$$\epsilon' = \epsilon_0\cos\theta \tag{6a}$$

$$\epsilon'' = \epsilon_0\sin\theta \tag{6b}$$

Similarly, if stress is

$$\sigma = \sigma_0\sin(\omega t + \theta + \delta' + \delta)$$

then

$$\sigma = \sigma'\sin\omega t + \sigma''\cos\omega t \tag{7}$$

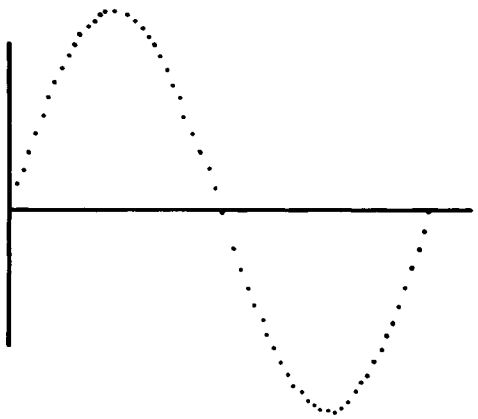

Fig. 1. Sixty-four data points on a sinusoidal signal.

and

$$\sigma' = \sigma_0 \cos(\theta + \delta + \delta') \tag{8a}$$

$$\sigma'' = \sigma_0 \sin(\theta + \delta + \delta') \tag{8b}$$

Similarly, for birefringence one can write

$$\Delta n' = \Delta n_0 \cos(\theta + \alpha + \alpha') \tag{9a}$$

$$\Delta n'' = \Delta n_0 \sin(\theta + \alpha + \alpha') \tag{9b}$$

where δ and α are the phase differences in the sample between stress–strain and birefringence–strain, respectively, and δ' and α' are the corresponding instrumental phase differences. α and δ can be determined after corrections for α' and δ' are applied.

In eq. (2) the Y_l's are the data points as shown in Figure 1. In eq. (2) in our studies m was chosen to be 64; however, it can be changed. Y_1^j represents various signals in the following manner:

$$Y_1^{1'} = \epsilon', \qquad Y_1^{1''} = \epsilon''$$

$$Y_1^{2'} = \sigma', \qquad Y_1^{2''} = \sigma''$$

$$Y_1^{3'} = \Delta n', \qquad Y_1^{3''} = \Delta n''$$

Using this terminology, modulus, stress-optical coefficient, and strain-optical coefficients are given by the following equation:

$$A_{ij} = \frac{Y_1^{i'} \cdot Y_1^{j'} + Y_1^{i''} \cdot Y_1^{j''}}{\left(Y_1^{j'}\right)^2 + \left(Y_1^{j''}\right)^2} + i\frac{Y_1^{j''} \cdot Y_1^{i'} - Y_1^{j'} \cdot Y_1^{i''}}{\left(Y_1^{j'}\right)^2 + \left(Y_1^{j''}\right)^2} \tag{10}$$

where $A_{21}^* =$ modulus (E^*), $A_{32}^* =$ stress-optical coefficient (C^*), and $A_{31}^* =$

strain-optical coefficient (K^*) and the loss tangents would be given by the following equation

$$\tan Q_{ij} = \frac{Y_1^{j''} \cdot Y_1^{i'} - Y_1^{j'} \cdot Y_1^{i''}}{Y_1^{i'} \cdot Y_1^{i'} + Y_1^{j''} \cdot Y_1^{i''}} \tag{11}$$

where Q_{21} = mechanical loss angle (δ), Q_{31} = phase difference between birefringence and strain (α), and Q_{32} = phase difference between birefringence and stress ($\alpha - \delta$).

Theoretically, higher order Fourier coefficients can be used to study the nonlinear viscoelastic nature of the material. If the departures from linear viscoelastic behavior are small, and, if one is using the analog signal for data analysis, the study of nonlinear viscoelastic behavior is difficult. But with digitized data and automated data acquisition techniques, one could collect data over a large number of cycles and thereby reduce the error. However, the accuracy would still be limited because of the resolution of the analog to digital converter and signal to noise ratio. If we apply a sinusoidal strain $\epsilon(t) = \epsilon_0 \sin \omega t$ to a sample, then under nonlinear viscoelastic response, stress, and birefringence would be given by the following equations:

$$\sigma(t) = \epsilon_0 [E'(\omega)\sin \omega t + E''(\omega)\cos \omega t + E'(2\omega)\sin 2\omega t + E''(2\omega)\cos 2\omega t + \cdots] \tag{12a}$$

$$\Delta n = \epsilon_0 [K'(\omega)\sin \omega t + K''(\omega)\cos \omega t + K'(2\omega)\sin 2\omega t + K''(2\omega)\cos 2\omega t + \cdots] \tag{12b}$$

where E', E'', K', and K'' are the real and imaginary parts of the modulus and strain optical coefficients, respectively. The modulus and other parameters calculated from higher order harmonics in Fourier series should compare with the same parameter obtained from the first order Fourier coefficients at the corresponding high frequency. However, such an analysis was not done on our present setup for the previously mentioned limitations. The work reported in this and the following paper was carried out during 1980–1981. Recently Tanaka et al.[26] have indeed used the Fourier analyses technique for nonlinear dynamic birefringence study on polymers.

Birefringence

The birefringence measurement is done using the method of optical transmission. For a nonscattering, nonabsorbing, birefringent sample, the fractional transmission for monochromatic light between crossed polarizers with their polarization axis at 45° to the optic axis of the sample is

$$T = \sin^2(\delta/2) \tag{13}$$

where δ is the retardation of the sample given by

$$\delta = 2\pi(d/\lambda)\Delta$$

for a sample of thickness d and birefringence Δ with light of wavelength λ. In the actual case some amount of absorbance, reflectance and transmittance is always present. Therefore, eq. (13) is modified as follows:

$$T = F\sin^2(\delta/2) + T_s \tag{14}$$

where F is the attenuation of the light beam resulting from reflection, absorption, and scattering which is given by

$$F = e^{-(k+\tau)d}(1 - r) \tag{15}$$

where k is the absorption coefficient, τ the turbidity, and r the reflectivity of the sample. The quantity T_s is the transmittance of the sample arising from (a) depolarization of the transmitted light resulting from the presence of locally birefringent structures such as spherulites and (b) the low angle light which can reach the photomultiplier tube and which is measured along with I_{trans} because of its admitting light diverging up to some finite angle. This term gives rise to transmission, even if there is no macroscopic birefringence and may change with elongation and consequently will vary during a dynamic birefringence experiment.

The quantity F may be estimated by measuring the transmittance of the sample with the analyzing polarizer removed. An approximate way to estimate T_s is to measure the transmittance when polarizer and analyzer are 0° and 90° to the optic axis.

If d_0 is the thickness of the sample in the unstrained state, (L/L_0) is the static draw ratio, and ϵ_0 is the amplitude of the dynamic strain ($\epsilon_0 \ll 1$), then thickness d at any time t during sinusoidal vibration can be approximated (under the assumption of constant volume deformation) according to the following equation:

$$d = d_0(L/L_0)^{-1/2}[1 - (\epsilon_0/2)\sin\omega t] \tag{16}$$

DESCRIPTION OF THE APPARATUS

A block diagram of the apparatus is given in Figure 2. It consists of an He–Ne laser, polarizer, compensator, analyzer, photomultiplier tube, sample chamber (heating and cooling arrangement), a JP series load cell (from Data Instruments Inc.), a DC–DC linear variable differential transformer (LVDT), encorder, belt and pulley system, amplifiers, analog to digital converter, microcomputer AIM 65 (Rockwell International), and oscilloscope. The encorder is used to send two types of pulses: (i) an index pulse (1 pulse per revolution) and (ii) 512 pulses per revolution. It is attached with the belt and pulley system in such a way so that the rotation frequency of the encorder and the vibration frequency of the sample are the same. The belt and pulley system is used to change the frequency. A series of cams was used to change the amplitude of the sinusoidal vibration. The strain signal from the linear variable differential transformer, the stress signal from the load cell, and the birefringence signal from the photomultiplier tube (PMT) are amplified. The

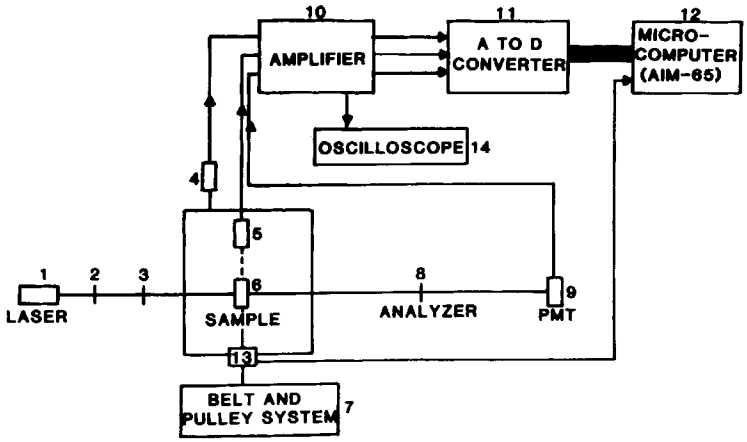

Fig. 2. Block diagram of the apparatus: (2) polarizer; (3) compensator; (4) LVDT; (5) load cell; (13) encorder.

amplified signals can either be seen on the oscilloscope or stored in the computer after it is digitized by an analog to digital converter. The A to D converter is a MDAS-8D from Datel Systems, Inc. Originally the AIM-65 microcomputer had 4K (byte) random access memory (RAM) which was extended to 36K (byte) RAM using a memory extension board (Model 6502 DM from Beta Computer Devices) of 32K. The AIM-65 microcomputer has a volatile memory; thus, to record the programs, a Radio Shack "Realistic" audio cassette tape recorder was used. For the purpose of dynamic birefringence experiments, two programs are written: (i) in assembly language for data acquisition [points Y_l's of eq. (2) are the data points] and (ii) in basic language for data analysis to determine A_{ij}'s of eq. (10) and tan Q_{ij}'s of eq. (11).

CALIBRATION

The calibration of the LVDT is done using a series of cams of known amplitude, and the load cell is calibrated by applying known weights to it. The calibration of PMT is relatively more difficult. As described previously, the transmittance of light varies according to eq. (14) as is pictorially shown in Figure 3. A, B, and C are three points on an approximately linear portion of the curve. For ease of analysis it will be best if the total retardation in the path of light oscillates within the limits of A and B. This is adjusted using the Berek compensator. If the total retardation of the sample at a given amplitude of vibration is such that the transmittance of light fluctuates more than AB, then calibration is relatively more complicated. To calibrate (within AB) PMT, known amounts of retardation are introduced using the Berek compensator and thus the slope of the line AB is determined.

As previously indicated, the encorder sends two types of pulses: (a) an index pulse, 1 pulse per cycle, and (b) 512 pulses per cycle. An index pulse is used at the beginning of the first cycle to instruct the computer when to start the data acquisition. For each of the three signals we are taking 64 data points per cycle. Thus, of the 512 pulses, data is taken on $64 \times 3 = 192$ pulses at equal

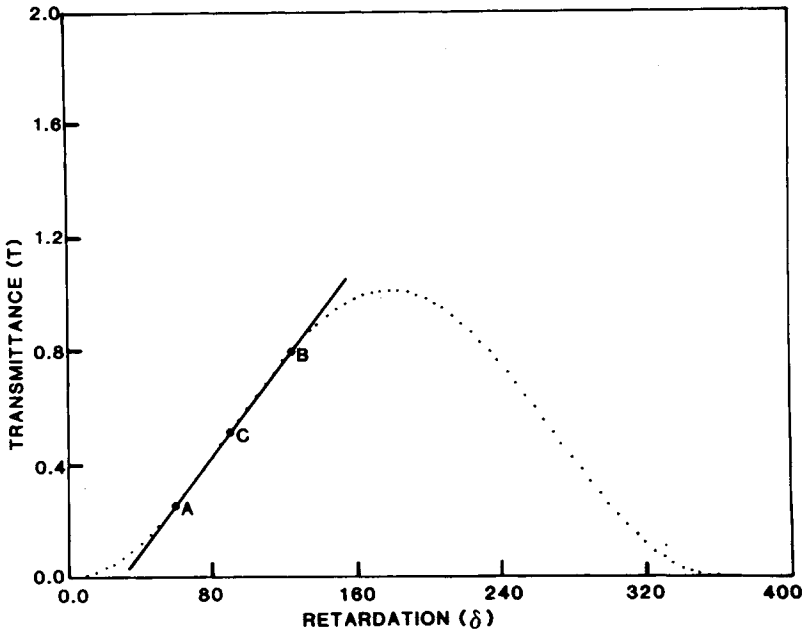

Fig. 3. Transmittance as a function of retardation.

intervals in each signal. At the first of the 512 pulses, strain, at the second pulse, stress, and at the third pulse, birefringence, are taken. The next five pulses are skipped. The second data points of strain, stress, and birefringence are taken at the 9th, 10th, and 11th pulses, respectively. In this way for $l = 1$ to 64, strain, stress, and birefringence signals are taken at the $[8(l-1)+1]$th, $[8(l-1)+2]$th, and $[8(l-1)+3]$th pulses, respectively. This data is averaged over the number of cycles. The measurements of the three signals are not simultaneous. The above mechanism of data acquisition introduces a phase difference of $2\pi/512$ between strain and stress, and that of $4\pi/512$ between strain and birefringence. The correction for these phase differences is necessary and has been done in our computer program. If σ_k^* and $\Delta\tilde{n}_k^*$ are the uncorrected Fourier coefficients of kth order in the equation of stress and birefringence, then their phase corrected values are given by the following equations:

$$\sigma_k^* = e^{-ik\cdot 2\pi/512} \cdot \tilde{\sigma}_k^* \tag{16a}$$

$$\Delta n_k^* = e^{-ik\cdot 4\pi/512} \cdot \Delta\tilde{n}_k^* \tag{16b}$$

In order to determine whether any other instrumental phase difference occurs in addition to the ones discussed above, two tests were conducted: (i) stress–strain data were collected for a steel spring at 0.6% sinusoidal strain and (ii) strain–birefringence data was collected for rubber strips at 0.6% sinusoidal strain. At these low levels of strain amplitude, it is expected that strain and stress would be in phase for the metallic strip and that strain and birefringence would be in phase for the rubber sample. The phase difference results for both of these tests are given in Figure 4, in terms of the values of δ

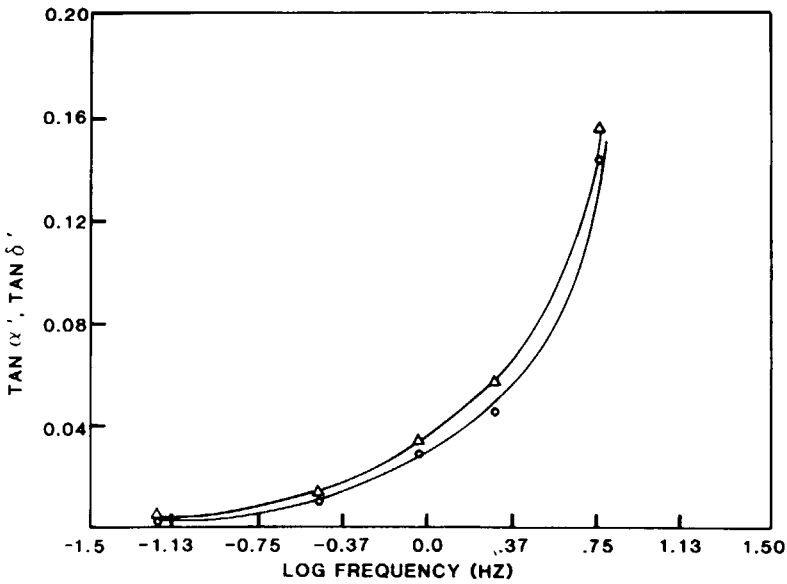

Fig. 4. Instrumental phase difference between (i) strain–stress ((△)δ') and (ii) strain–birefringence ((○)α').

and α by which strain lags stress and birefringence. These values arise essentially because of the response time of the LVDT, and correction for which is applied to the experimental data. This apparatus was used to study the molecular motion in acrylonitrile copolymers. Results of this study are reported in a separate publication.[25]

The support of the Army Research Office (Durham), the National Science Foundation, and the Standard Oil Co. (Ohio) in this work is gratefully acknowledged. We also recognize the preliminary considerations of this apparatus by Dr. William Mead as well as many useful discussions with Dr. Shoji Suehiro (of Kyoto University). Technical assistance of Mr. Norman Page and John Domian is also appreciated.

References

1. R. S. Stein, *J. Polym. Sci.*, **62**, S2 (1962).
2. T. Hashimoto, R. E. Prud'homme, D. A. Keedy, and R. S. Stein, *J. Polym. Sci., Polym. Phys. Ed.*, **11**, 693 (1973); T. Hashimoto, R. E. Prud'homme, and R. S. Stein, *ibid.*, 709 (1973).
3. G. D. Patterson, *Polym. Prepr. Am. Chem. Soc.*, **22**(2), 265 (1981).
4. H. Kawai, T. Itoh, D. A. Keedy, and R. S. Stein, *J. Polym. Sci., Polym. Lett. Ed.*, **2**, 1075 (1964).
5. A. Tanaka, E. P. Chang, B. Delf, I. Kimura, and R. S. Stein, *J. Polym. Sci., Polym. Phys. Ed.*, **11**, 1891 (1973).
6. T. Kyu, M. Yamada, S. Suehiro, and H. Kawai, *Polym. J.*, **12**, 809 (1980).
7. S. L. Hsu and D. J. Burchell, *Polym. Prepr. Am. Chem. Soc.*, **22**(1), 305 (1981).
8. G. Bayer, W. Hoffmann, and H. W. Siesler, *Polymer*, **21**(2), 235 (1980).
9. R. S. Stein, S. Onogi, and D. A. Keedy, *J. Polym. Sci.*, **57**, 801 (1962).
10. R. S. Stein, S. Onogi, K. Sanguri, and D. A. Keedy, *J. Appl. Phys.*, **34**, 80 (1963).
11. K. Sanguri and R. S. Stein, *J. Polym. Sci.*, **C5**, 139 (1963).
12. R. Yamada and R. S. Stein, *J. Appl. Phys.*, **36**(10), 3005 (1965).
13. A. Takeuchi and R. S. Stein, *J. Polym. Sci., A-2* **5**, 1079 (1967).

14. B. E. Read, *Techniques of Polymer Science*, SCI Monographs No. 17, Society of the Chemical Industry, London, 1963, p. 198.
15. B. E. Read, *J. Polym. Sci.*, **C5**, 87 (1964).
16. B. E. Read, *Polymer*, **1**, 5 (1964).
17. B. E. Read, *J. Polym. Sci.*, **C16**, 1887 (1967).
18. B. E. Read, *Polymer*, **22**, 1580 (1981).
19. J. F. Rudd, *J. Polym. Sci., Polym. Lett. Ed.*, **3**, 345 (1965).
20. D. G. LeGrand and P. F. Erhardt, *Trans. Soc. Rheol.*, **6**, 301 (1962).
21. B. H. Zimm, *Rev. Sci. Instrum.*, **29**(5), 360 (1958).
22. P. L. Frattini and G. G. Fuller, *J. Rheol.*, **28**(1), 61 (1984).
23. D. G. LeGrand, *J. Polym. Sci.*, **A2**, 931 (1964).
24. T. Kyu, N. Yamada, M. Tabushi, S. Nomura, and H. Kawai, *Polym. J.*, **7**, 108 (1975).
25. S. Kumar, W. T. Mead, and R. S. Stein, *J. Appl. Polym. Sci.*, **34**, 1703 (1987).
26. A. Tanaka, private communications.

Received December 5, 1986
Accepted February 23, 1987